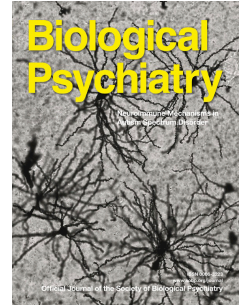# Journal Pre-proof

Reduced neuronal cAMP in the nucleus accumbens damages blood-brain barrier integrity and promotes stress vulnerability

Yue Zhang, Wuhuan Lu, Zibin Wang, Ran Zhang, Yuan Xie, Suhan Guo, Li Jiao, Yu Hong, Zizhen Di, Jiye Aa, Guangji Wang

Please cite this article as: Zhang Y., Lu W., Wang Z., Zhang R., Xie Y., Guo S., Jiao L., Hong Y., Di Z., Aa J. & Wang G., Reduced neuronal cAMP in the nucleus accumbens damages blood-brain barrier integrity and promotes stress vulnerability, *Biological Psychiatry* (2019), doi: https://doi.org/10.1016/j.biopsych.2019.09.027.

This is a PDF file of an article that has undergone enhancements after acceptance, such as the addition of a cover page and metadata, and formatting for readability, but it is not yet the definitive version of record. This version will undergo additional copyediting, typesetting and review before it is published in its final form, but we are providing this version to give early visibility of the article. Please note that, during the production process, errors may be discovered which could affect the content, and all legal disclaimers that apply to the journal pertain.

1   **Reduced neuronal cAMP in the nucleus accumbens damages blood-brain barrier integrity**

2   **and promotes stress vulnerability**

3

4   Yue Zhang[1], Wuhuan Lu[1], Zibin Wang[2], Ran Zhang[1], Yuan Xie[1], Suhan Guo[1], Li Jiao[1], Yu Hong[1],

5   Zizhen Di[3], Jiye Aa[1]*, Guangji Wang[1]*

6

7   1. Key Laboratory of Drug Metabolism and Pharmacokinetics, State Key Laboratory of Natural

8   Medicines, China Pharmaceutical University, No. 24 Tongjia Lane, Nanjing, 210009, China.

9   2. Analytical and Testing Center, Nanjing Medical University, No. 101 Longmian road, Nanjing,

10   211166, China.

11   3. Liaoning Provincial Academy of Traditional Chinese Medicine, No. 60 Huanghe North Street,

12   Shenyang, 110034, China.

13

14   *Correspondence to Jiye Aa (Email: jiyea@cpu.edu.cn), Tel:(+86)2583271081, Fax:

15   (+86)2583271060; Guangji Wang (guangjiwang@hotmail.com), Tel: (+86) 2583302827, Fax:

16   (+86) 2583302827. Key Laboratory of Drug Metabolism and Pharmacokinetics, China

17   Pharmaceutical University, Nanjing, 210009, China.

18

19   Running title: **Reduced cAMP in the NAc damages BBB integrity**

20

21

22

1

2

Abstract:

Background: Studies have suggested that chronic social stress specifically downregulates endothelial tight junction protein expression in the nucleus accumbens (NAc), thus increasing blood-brain barrier (BBB) permeability and promoting depression-like behaviors. However, the molecular mechanism underlying the reduction in tight junction protein, particularly in the NAc, is largely uncharacterized.

Methods: We performed comparative metabolomic profiling of the nucleus accumbens, prefrontal cortex and hippocampus of social defeat-stressed mice to identify the molecular events that mediate BBB breakdown.

Results: We identified the levels of cAMP were specifically reduced in the NAc and positively correlated with the degree of social avoidance. Replenishing cAMP in the NAc was sufficient to improve BBB integrity and depression-like behaviors. We further found that cAMP levels were markedly decreased in neurons of the NAc, rather than in endothelial cells, astrocytes or microglia. RNA-Seq data showed that adenylate cyclase 5 (Adcy5), an enzyme responsible for the synthesis of cAMP from ATP, was predominantly expressed in the NAc and exclusively resided in neurons. Endogenous modulation of cAMP synthesis in neurons through the knockdown of Adcy5 in the NAc regulated the sensitivity to social stress. Moreover, deficient neuronal cAMP production in the NAc decreased the expression of reelin, while supplementary injection of exogenous reelin into the NAc promoted BBB integrity and ameliorated depression-like behaviors.

Conclusions: Chronic social stress diminished cAMP synthesis in neurons, thus damaging BBB

1   integrity in the NAc and promoting stress vulnerability. These results characterize

2   neuron-produced cAMP in the NAc as a biological mechanism of neurovascular pathology in

3   social stress.

4

5   Keywords: social stress, metabolomics, nucleus accumbens (NAc), cAMP, blood-brain barrier

6   (BBB), stress vulnerability

7

8

9

10 **Introduction**

11 Major depression is a common illness, with a lifetime risk of approximately 15~18%

12 worldwide(1, 2). Shortcomings in the effectiveness of now-available antidepressant treatments

13 have resulted in an enormous public health burden of depression(3, 4). Cumulative studies have

14 outlined that inflammation appears to precede depression(5), and patients diagnosed with major

15 depressive disorder (MDD) have higher levels of circulating pro-inflammatory cytokines(6, 7).

16 Peripheral inflammation can activate microglia and immune cells embedded in the brain, thereby

17 disrupting the plasticity and development of nerve cells(6, 8).

18 Emerging evidence suggests that peripheral monocytes cannot infiltrate the brain parenchyma

19 of stress-susceptible mice, but accumulate at the endothelial surface and perivascular space,

20 thereby resulting in vascular remodeling(9-12). A previous study outlined that social stress

21 specifically alters blood-brain barrier (BBB) integrity in the nucleus accumbens (NAc) through

22 downregulation of endothelial tight junction protein Cldn5(11). NAc is a crucial region within the

1   brain's reward circuitry(13, 14). Increased permeability of the BBB tends to appear at the NAc,

2   indicating a more complicated mechanism that mediates neurovascular remodeling in stressed

3   mice. However, the molecular mechanism under which endothelial tight junction protein is

4   particularly downregulated in the NAc of stress-susceptible mice is so far unclear. Herein, we

5   identified a specific reduction in the levels of cAMP in the NAc through comparative

6   metabolomics analysis. The data suggested that neuronal cAMP in the NAc orchestrates BBB

7   integrity and the resultant effects on depression-like behaviors through a reelin mediated

8   extracellular matrix network. Our study thus extends the understanding of BBB breakdown in the

9   NAc associated with chronic social stress, providing a new perspective for understanding

10   neurovascular pathology in depression.

11

12

13   **Methods and Materials**

14

15   **Animals**

16   Male C57BL/6J mice (7-8 weeks of age) and male CD-1 mice (retired breeders, 4-6 months of age)

17   were used (Vital River Laboratories, Beijing, China). C57BL/6J mice were housed five per cage

18   and CD-1 mice were singly housed under standard laboratory conditions with a 12-h light-dark

19   cycle (lights were on from 7 a.m. to 7 p.m.), temperature ($24\pm1\,^{\circ}\mathrm{C}$), food and water *ad libitum*. The

20   mice were acclimated for a minimum of 7 d prior to experiment initiation. All animal experimental

21   procedures were approved by the Animal Ethics Committee of China Pharmaceutical University

22   and performed in accordance with the US National Institutes of Health Guidelines.

1

2 **Social defeat stress model**

3 **Chronic social defeat stress (CSDS)**

4

5   Ten-day chronic social defeat stress was performed as previously described(15). Briefly,

6 aggressive CD-1 mice were selected by a 3-d screening process. During the 10-d defeat period,

7 each intruder C57BL/6J mouse was exposed to a novel resident aggressive CD-1 mouse to be

8 physically defeated for 10 min on 10 consecutive days. Then, the intruder was transferred to

9 one-half of the cage (the opposite compartment separated by a perforated Plexiglas divider) to

10 maintain sensory contact for the remainder of the 24-h period. Control C57BL/6J mice were pair

11 housed in the home cage, one mouse per side of the perforated Plexiglas divider to avoid physical

12 contact with their cage mates. Social interaction test was performed 24 h after the last defeat.

13 **Microdefeat stress**

14   The microdefeat protocol is a variant of the chronic social defeat protocol, as previously

15 described(16). Experimental C57BL/6J mice were subjected to subthreshold levels of social defeat

16 to evaluate the increased susceptibility to stress. Three consecutive 5-min defeat sessions were

17 conducted within the same day with 15 min of rest between each bout. Social interaction was

18 tested 24 h later.

19

20 **Behavioral assays**

21 **Social interaction test**

22   Social interaction (SI) test was performed as previously described with minor modifications(15).

First, the mice were adapted to the environment of the experimental room for more than 30 min.

Then, the mice were placed in an open-field arena (40 cm× 40 cm× 40 cm), containing a small

wire animal cage placed on one side. Social avoidance behavior was measured according to a

two-stage social interaction test, recorded with a Logitech camera (C170) and analyzed by

Any-maze software (Global Biotech Inc.). In the first stage, the behavior of C57BL/6J mice was

recorded for 150 s, without a CD-1 aggressor in the interaction zone. At the end of this stage, the

mouse was removed for 30 s, and the arena was cleaned. In the second stage, the same metrics

were measured, with a novel CD-1 aggressor in the interaction zone. The social interaction ratio

(SI ratio) was calculated by dividing the time spent in the interaction zone with the target by the

time spent in the interaction zone without the target. Mice were deemed to be susceptible (SI ratio

<1) or resilient (SI ratio >1).

Forced swim test (FST)

Experimental mice were singly placed in a 5-L glass beaker (17.8 cm diameter, 27.5 cm height)

containing 18-20 cm of water (23-25 ℃) and videotaped for 6 min under normal light(17). The

immobility time was measured for the last 4 min by two colleagues who were blinded to the

experiment. A stop watch was used to calculate the active behavior (swimming and climbing), and

the rest immobility time was analyzed.

Tail suspension test (TST)

Experimental mice were individually suspended by the tails with adhesive tape in the tail

suspension box, roughly 20 cm above the ground and blinded to each other. The animals were

video-recorded for 6 min, and the time of immobility was quantitated over the last 4 min by two

colleagues who were blinded to the experiment. Immobility was defined as no movement at all or

1   only minor limb movements.

2   **Sucrose preference test (SPT)**

3   The sucrose preference test was performed during the dark period, started with an adaptive

4   phase to water and 1% sucrose for 24 h, during which the two bottles were switched every 12 h.

5   After water deprivation for 12 h, all bottles were weighed and mice were individually housed with

6   free access to water or 1% sucrose for a 12-h period. The bottles were then reweighed and the

7   sucrose preference was calculated by dividing the amount of sucrose consumed by the total liquid

8   weight consumed.

9

10   **Metabolomics study and multivariate statistical analysis**

11   The metabolomics study of the samples, e.g., brain tissues of the mice, was performed based on

12   a well-developed GC-MS and LC-MS/MS platform, as previously reported(18-20). The details

13   regarding sample preparation, derivatization, chromatography conditions and detection of the

14   analytes for GC-MS and LC-MS/MS can be found in the supplemental information.

15

16   ***In vivo* exposure of meglumine cAMP in mice and drug treatments**

17   To evaluate the plasma and brain (NAc) distribution of meglumine cAMP, mice were

18   intraperitoneally administered meglumine cAMP (10 mg/kg, dissolved in 0.9% saline) or 0.9%

19   saline as a control. 100 μL blood samples (collected from ophthalmic veins) and NAc tissues were

20   collected at 30 min, 1, 2, 4, 6, 12 and 24 h. The collected blood samples were centrifuged at 8,000

21   g for 5 min. The supernatant and the brain tissues were immediately stored at -70 ℃ until further

22   analysis. The concentration of cAMP in the plasma and NAc tissue was determined using a cAMP

1 ELISA kit.

2 To examine the prophylactic effect of meglumine cyclic adenylate (M-cAMP) supplementation,

3 M-cAMP (10 mg/kg, dissolved in 0.9% saline) was intraperitoneally (i.p.) administered 2 h prior

4 to the social defeat, once daily for 10 d during the CSDS. Behavioral tests were performed 24 h

5 after the last M-cAMP administration. To examine the effect of NAc supplement of M-cAMP,

6 selected susceptible mice were anesthetized with isoflurane (4% for induction, followed by 1% for

7 maintenance, MSS Int. Ltd, UK) and positioned in a stereotaxic instrument (RWD Life Science).

8 Bilateral NAc (bregma coordinates: anteroposterior +1.6 mm, mediolateral ± 1.4 mm,

9 dorsoventral   –4.4 mm) were infused with 0.5 μL M-cAMP or saline at a rate of 0.1 μL/min(11,

10 21). Social interaction tests were performed on day 1, 4 or 7 after injection. TST and FST were

11 respectively performed on day 8 and 9 after injection.

12 For reelin supplementation, recombinant mouse reelin (0.5 μg/μL, 0.75 μL, 3820-MR-025,

13 R&D Systems)(22, 23) or vehicle (1% bovine serum albumin in sterile PBS) was stereotactically

14 injected into the NAc bilaterally, using the above mentioned coordinates for the NAc. Microdefeat

15 stress and behavioral tests were performed three days after the injection.

16 For the fluoxetine treatment, unstressed controls and selected susceptible mice were randomly

17 divided into either vehicle or fluoxetine (10 mg/kg, daily i.p. administration) treatment groups.

18 NAc tissues were collected either on day 5 or 35 for western blot analysis.

19

20 **Stereotaxic surgery and viral gene transfer**

21 For bilateral stereotaxic injection, mice were anesthetized with isoflurane and placed in a fixed

22 position in the small-animal stereotaxic instrument (RWD Life Science). The coordinates of NAc

1   were located according to the bregma: anteroposterior +1.6 mm, mediolateral $\pm$1.4 mm, and

2   dorsoventral -4.4 mm. Each side of NAc was infused with 0.5 μL virus (AAV2/9-shRNA or

3   AAV2/9-shRNA-Adcy5, $2.38\lozenge10^{12}$ v.g./mL, $2.02\lozenge10^{12}$ v.g./mL, respectively) at a rate of 0.1

4   μL/min, and the needle was retained for 10 min before removal. The mice were post hoc screened

5   according to the expression of GFP.

6

7   **Immunofluorescence**

8   Mice were transcardially perfused with cold saline, and brains were postfixed and sectioned.

9   More details are described in the supplemental information.

10

11   **Capillary extraction and ELISA measurement**

12   The blood vessels of the NAc were isolated as previously described (11, 24), and more details

13   are described in the supplemental information.

14

15   **Transmission electron microscopy (TEM)**

16   TEM experiments were performed as described in the supplemental information.

17

18   **RNA sequencing, real-time quantitative PCR**, **and western blot analysis**

19   The complete details of RNA sequencing, real-time quantitative PCR, and western blot analysis

20   are provided in the supplemental information.

21

22   **Statistical analysis**

1   Behavioral experiments and analyses were performed by colleagues blinded to the treatment

2   assignments. Mice were randomly grouped and the number of replicates is indicated by the dots in

3   the figures or in the figure legends. The values that were greater than 2 s.d. from the mean were

4   identified as outliers and excluded from further statistics. All experimental data are presented as

5   the mean ± s.e.m. Statistical analyses were performed using GraphPad Prism 7.0 software.

6   Differences between two groups were examined by the unpaired Student's *t*-test. Differences

7   among multiple groups were evaluated using one-way ANOVA or two-way ANOVA followed by

8   Bonferroni's *post hoc* comparisons. *P*<0.05 was considered statistically significant. Correlations

9   were assessed with Pearson's correlation coefficient or Spearman correlation coefficient. The

10   incidence of depression susceptibility was analyzed with Fisher's exact test. Heatmaps were

11   performed using R and visual representation of mean values. A summary of the statistical analyses

12   is listed in Table S1.

13

14   **Data availability**

15   The datasets are available from the corresponding author upon request.

16

17   **Results**

18   **Social stress vulnerability is associated with reduced cAMP in the NAc**

19   Reduced expression of the tight junction protein Cldn5 in the NAc was shown to alter BBB

20   integrity, thus promoting depression-like behaviors; however, Cldn5 expression and BBB integrity

21   were shown to remain unchanged in the prefrontal cortex (PFC) and hippocampus (Hip.)(11).

22   Consistent with this finding, we observed an intense and persistent increase of IL-6 levels in the

10

1   plasma and NAc of the susceptible (SS) mice 24 h after the social interaction (SI) test (Figure

2   S1A-S1E), and further verified the downregulation of Cldn5 in the NAc (Figure S1F). No

3   difference was observed of IL-1β and TNF-α levels in the brain despite a slight increase in plasma

4   (Figure S1E). To characterize the molecular mechanisms that underlie the region-specific

5   breakdown of BBB integrity in the NAc, we performed comparative metabolomic profiling of the

6   three candidate sites (NAc, PFC and Hip.) involving impaired functions in MDD of unstressed

7   control (CTRL), susceptible (SS) and resilient (RES) mice after a 10-d chronic social defeat stress

8   (CSDS) (Figure 1A-1D). Metabolome analyses can be employed to discover pathogenesis

9   biomarkers for diseases, such as cardiovascular disease(25), dyslipidemia(26), cancer(27), and

10   Alzheimer's disease(28). Here, a total of 255 endogenous metabolites were detected by GC-MS

11   and LC-MS/MS. Figure 1E shows the differential metabolites specifically varied in the NAc of SS

12   mice compared to those in the CTRL and RES mice, while no significant difference of these

13   metabolites was observed in the PFC or hippocampus. Figure 1F is a heatmap showing the

14   correlation of the concentration of these metabolites with the SI ratio. Notably, the level of cAMP

15   was significantly lower in the NAc of SS mice (Figure 1G) and positively correlated with the

16   degree of social avoidance (Figure 1H). Similar data were obtained using an ELISA-based

17   approach (Figure 1I). Furthermore, the cAMP concentration in the NAc was higher than that in the

18   PFC or hippocampus. Together, these results suggest that the distinctive change in cAMP in the

19   NAc may underlie depression-like behaviors.

20

21   **cAMP supplementation improves blood-brain barrier and depressive-like behaviors**

22   To test whether replenishing cAMP could improve depressive behaviors, we examined the effects

1 of meglumine cyclic adenylate (M-cAMP) pretreatment (Figure 2A-2E). M-cAMP is a clinical

2 drug used for cardiovascular treatment that can readily cross cell membranes. To evaluate the

3 kinetics of daily i.p. M-cAMP treatment, we quantified the plasma levels and brain distribution of

4 cAMP after a single dose of 10 mg/kg M-cAMP. We verified that the levels of cAMP in

5 circulation and the NAc were sharply increased up to 6 h post injection, but not 12 and 24 h

6 (Figure 2F-2G). In the social interaction test, M-cAMP-pretreated mice exhibited higher SI ratios

7 (Figure 2B) and a lower incidence of depression susceptible than vehicle-treated mice after the

8 10-d social defeat stress (Figure 2C, Fisher's exact test, P=0.0033). In the TST and FST, M-cAMP

9 pretreatment significantly reduced the immobility time (Figure 2D-2E), indicating that cAMP had

10 antidepressant-like effects. The spatial overlap between the BBB leakage and decreased cAMP

11 levels specific in the NAc implied an association, but not necessarily a cause-and-effect. Herein, to

12 examine whether M-cAMP pretreatment affected the BBB permeability of the NAc, we detected

13 Cldn5 expression by immunofluorescence colocalization with CD31 and BBB leakiness by the

14 infiltration of Evans Blue (EB). Pretreatment with M-cAMP rescued Cldn5 expression (Figure

15 2H-2I), and M-cAMP-pretreated mice displayed no distinct infiltration of EB in the NAc (Figure

16 2J).

17   To further confirm the effect of cAMP in the NAc on depressive behaviors, we performed

18 stereotactic intra-NAc injection of M-cAMP or saline-vehicle to the susceptible mice (Figure 2K).

19 A single intra-NAc injection of M-cAMP gradually improved the social avoidance behavior within

20 one week (Figure 2L), and significantly reduced the immobile time in the TST and FST assays

21 (Figure 2M-2N). These results support the hypothesis that replenishing cAMP in the NAc

22 facilitates BBB integrity and induces antidepressant-like effects.

1

cAMP is markedly decreased in neurons of the NAc in stress-susceptible mice

cAMP is thought to promote the functions of tight junctions in endothelial cells *in vitro*(29, 30).

As a second messenger, the synthesis and functioning of cAMP are restricted within the cell. To

determine whether cAMP was decreased in blood vessels, thus mediating the downregulation of

Cldn5, we next enriched the blood vessels of the NAc using a brain capillary extraction method.

After capillary extraction, the vascular sections formed a pellet in the bottom, with myelin debris

floating at the surface, and both of which were separately collected for measuring cAMP

concentration. Unexpectedly, no difference was detected for cAMP levels in NAc blood vessels of

SS mice when compared to control and RES mice (Figure 3A). However, the cAMP level in the

myelin debris of SS mice was significantly attenuated, and the cAMP level in the myelin debris of

the NAc was remarkably correlated with the degree of social avoidance (Figure 3B). To further

determine the cell type that mediates the decreasing of cAMP, we performed the

immune-colocalization analysis. Immunostaining revealed that cAMP was precisely colocalized

with the neurons and markedly decreased in neurons in the NAc, but not in astrocytes or microglia

(Figure 3C-3E).

  cAMP is synthesized from ATP by adenylate cyclase located on the inner side of the plasma

membrane and degraded to AMP by phosphodiesterase enzymes. Along with the reduction of

cAMP (Figure S2A), the metabolomic profiling also revealed that ATP was accumulated (Figure

S2B), while AMP was constant in the NAc of SS mice (Figure S2C), indicating that the activity of

adenylate cyclase was disturbed in the NAc. Our RNA-sequencing (RNA-seq) data displayed that

the NAc region predominantly expressed adenylate cyclase 5 (*Adcy5*) among the 10 subtypes

1   (Figure 3F). Moreover, a single cell RNA sequencing of the mouse nervous system mapped that

2   *Adcy5* was mainly expressed in the medium spiny neurons of the NAc (Figure S2D)(31). Adenylyl

3   cyclase is activated by coupling with Gsα, especially the Gsα located in nonlipid raft region,

4   where it is more facile to activate adenylyl cyclase(32, 33). We next explored the protein

5   expression of Adcy5 and Gsα both in lipid raft region and non-raft region, using flotillin-1 as a

6   neuron specific lipid raft marker. No difference of protein expression of Adcy5 was observed in

7   either the lipid raft or non-raft region, however, Gsα expression was markedly dampened in

8   non-raft region of SS mice, mediating a reduced ability of Adcy5 to convert ATP to cAMP in the

9   NAc (Figure 3G-3H).

10   Taken together, these results demonstrated that the lessened cAMP in the NAc of SS mice was

11   occurred in the neurons, and was mediated by less Gsα translocation from lipid rafts to non-raft

12   region.

13

14   **Behavioral changes following endogenous modulation of neuronal cAMP synthesis in the**

15   **NAc**

16   To further confirm the causal role of cAMP in social stress induced depressive behaviors, we

17   conducted conditional knockdown of Adcy5 to modulate the neuronal cAMP concentration in the

18   NAc *in vivo*. A doxycycline-inducible adeno-associated virus (AAV 2/9 serotype) targeting shRNA

19   transcripts encoding *Adcy5* allows for reversible modulation of cAMP in the NAc (Figure S3A).

20   We confirmed the downregulation of *Adcy5* mRNA and protein, as well as lower cAMP levels in

21   the NAc (Figure S3B-S3G). No difference was found for other subtypes of adenylate cyclase.

22   After 2 weeks of recovery followed by 2 weeks of treatment with doxycycline, the microdefeat, a

1   subthreshold level of social defeat, was employed to investigate the pro-susceptibility effect of

2   reductive cAMP in the NAc (Figure 4A). We consistently observed that the reduction in cAMP

3   alone had no effect on the behaviors, however, the cAMP reduction in combination with exposure

4   to microdefeat markedly induced social avoidance behavior and anhedonia (Figure 4B-4C, Figure

5   S4A-S4B). Notably, withdrawal of doxycycline in the following 5 days, allowing recovery of

6   *Adcy5* expression (Figure S3H-S3K), significantly reversed the depressive behaviors (Figure

7   4D-4F, Figure S4C). Moreover, another cohort of mice conducted replenishing cAMP also

8   displayed insusceptible to the microdefeat (Figure 4G-4L, Figure S4D-S4F). Together, these

9   results suggest that neuronal cAMP deficiency in the NAc enhanced stress susceptibility in mice.

10

11   **Reelin mediates the antidepressant-like effects of cAMP**

12   The RNA-seq analysis indicated that the extracellular matrix (ECM)-receptor interaction

13   pathway was markedly disturbed in the NAc of SS mice compared to that in CTRL mice after a

14   10-d CSDS (Figure S5A). Among the genes in this pathway, the gene expression of collagen IV

15   (*Col IV*), which is the major structural component of basement membranes, was significantly

16   reduced. Colocalization of Col IV with CD31 and transmission electron microscopy showed that

17   the basement membrane of the BBB, not just endothelial tight junctions, was compromised in the

18   NAc (Figure S5B-S5C), while replenishing cAMP improved the integrity of the basement

19   membrane in the NAc (Figure S5D). Reelin (Reln), a secreted glycoprotein mainly expressed by

20   GABAergic interneurons, has been demonstrated to play a vital role in the extracellular matrix

21   network that promotes BBB development through astrocytic endfeet attachment to the vasculature

22   (34, 35). Notably, the expression of *Reelin* in the cerebrum was spatially coincided with *Adcy5*,

15

1   according to the Allen Brain Atlas (Figure S6). We therefore further examined whether the cAMP

2   level in the NAc potentially impacted the reelin signal. Interestingly, we found that the mRNA and

3   protein expression of reelin was much lower in AAV-shRNA-Adcy5 mice than in AAV-shRNA

4   mice (Figure 5A-5B), suggesting a crucial role of reelin in the cAMP deficiency mediated

5   pro-susceptibility. Peripheral IL-6 (~21 kDa) was reported to be able to penetrate the NAc

6   parenchyma of SS mice. We concomitantly found that the recombinant biotinylated IL-6 was

7   detectable in the NAc of stressed AAV-shRNA-Adcy5 mice, but not stressed AAV-shRNA mice

8   (Figure 5C). Notably, intra-NAc injection of reelin to the AAV-shRNA-Adcy5 mice was sufficient

9   to ameliorate social avoidance behavior in SI test (Figure 5D-5F) and anhedonia behavior in the

10   sucrose preference test (Figure 5G), as well as the infiltration of biotinylated IL-6 in the NAc

11   (Figure 5H). We also evaluated the effect of acute (5 d) and chronic (35 d) fluoxetine treatment on

12   the reelin signal in the NAc of SS mice. Chronic fluoxetine treatment (Figure 5J) but not acute

13   fluoxetine treatment (Figure 5I) was sufficient to recuperate reelin protein expression in the NAc.

14

15   **Discussion**

16

17   In general, our data suggest that neuronal cAMP in the NAc orchestrates BBB integrity and

18   stress vulnerability. cAMP was reported to be diminished globally in the brains of patients with

19   major depressive disorder (MDD) and was upregulated by antidepressant treatment(36, 37).

20   However, our current knowledge of cAMP in MDD, especially in some particular brain regions, is

21   fairly limited (38). Our findings complement previous evidence suggesting that replenishing

22   cAMP can ameliorate the BBB integrity of the NAc of stress-susceptible mice. BBB leakiness in

1   depression was first brought up several decades ago(39), and the most recent developments

2   highlighted that the BBB integrity of stress-susceptible mice was specifically compromised in the

3   NAc(11). Moreover, peripheral monocytes cannot infiltrate the brain parenchyma, but accumulate

4   at the endothelial surface and perivascular space(9, 10). Small molecules and proteins up to ~69

5   kDa have been reported to pass through the leaky BBB of stress-susceptible mice(11). The

6   extracellular matrix signal, also identified to be related to depression by some reports(40-43), has

7   been widely studied for its promotion of neurogenesis(44), modulation of synaptic plasticity(45),

8   and relation to cognitive deficits(46). Our work uncovers the molecular mechanism by which

9   neuronal cAMP may regulate the BBB integrity of the NAc via reelin-mediated extracellular

10 matrix signals.

11   A previous study focusing on the cAMP homeostasis regulated by the downstream

12 phosphodiesterase-4 (PDE4) pathway also confirmed the pivotal role of cAMP in NAc mediated

13 depression-like behaviors (47). Given that the present metabolomic profiling results supported that

14 the upstream but not downstream of cAMP synthesis was disturbed in the NAc, we thus addressed

15 the *Adcy5* mediated synthesis process of cAMP in the NAc. To our knowledge, an *in vitro* study

16 showed that ketamine produced antidepressant effect by increasing cAMP in glial cells and

17 astrocytes, rather than targeting NMDA receptors (48). This hints the crucial role of cAMP in

18 depression and the different effects of cAMP in particular cell types. Considering that *Adcy5* is

19 predominantly expressed in neurons, but also non-neurons to a minor extent, and that the viral

20 manipulation is not cell specific, further work is required to illuminate the specific groups of

21 neurons in the NAc that are involved in cAMP-mediated stress vulnerability. Overall, it is

22 plausible that replenishing cAMP in the NAc or targeting the regulation of endogenous cAMP

1　may promote the design of effective antidepressant drugs. In addition, it is interesting to note that

2　M-cAMP is a clinical drug for cardiovascular treatments, while depression and cardiovascular

3　disease have been found with high comorbidity in patients(49-51). A greater understanding of the

4　mechanisms by which M-cAMP enhances vascular health in MDD may promote the augmentation

5　of current treatment protocols.

6

15

16　**Disclosures**

17　The authors report no biomedical financial interests or potential conflicts of interest.

18

19　**References**

20

21　1.　Bromet E, Andrade LH, Hwang I, Sampson NA, Alonso J, de Girolamo G, *et al.* (2011):

22　Cross-national epidemiology of DSM-IV major depressive episode. *BMC Med* 9:90.

2. Disease GBD, Injury I, Prevalence C (2018): Global, regional, and national incidence, prevalence, and years lived with disability for 354 diseases and injuries for 195 countries and territories, 1990-2017: a systematic analysis for the Global Burden of Disease Study 2017. *Lancet* 392:1789-1858.

3. Krystal JH, Abdallah CG, Sanacora G, Charney DS, Duman RS (2019): Ketamine: A Paradigm Shift for Depression Research and Treatment. *Neuron* 101:774-778.

4. Patel V, Chisholm D, Parikh R, Charlson FJ, Degenhardt L, Dua T, *et al.* (2016): Addressing the burden of mental, neurological, and substance use disorders: key messages from Disease Control Priorities, 3rd edition. *Lancet* 387:1672-1685.

5. Jeon SW, Kim YK (2017): Inflammation-induced depression: Its pathophysiology and therapeutic implications. *J Neuroimmunol* 313:92-98.

6. Bullmore E (2018): Inflamed depression. *Lancet* 392:1189-1190.

7. Dantzer R, O'Connor JC, Freund GG, Johnson RW, Kelley KW (2008): From inflammation to sickness and depression: when the immune system subjugates the brain. *Nat Rev Neurosci* 9:46-56.

8. Husain MI, Strawbridge R, Stokes PR, Young AH (2017): Anti-inflammatory treatments for mood disorders: Systematic review and meta-analysis. *J Psychopharmacol* 31:1137-1148.

9. Pearson-Leary J, Eacret D, Chen R, Takano H, Nicholas B, Bhatnagar S (2017): Inflammation and vascular remodeling in the ventral hippocampus contributes to vulnerability to stress. *Transl Psychiatry* 7:e1160.

10. Weber MD, Godbout JP, Sheridan JF (2017): Repeated Social Defeat, Neuroinflammation, and Behavior: Monocytes Carry the Signal. *Neuropsychopharmacology*

42:46-61.

11. Menard C, Pfau ML, Hodes GE, Kana V, Wang VX, Bouchard S, *et al.* (2017): Social stress induces neurovascular pathology promoting depression. *Nat Neurosci* 20:1752-1760.

12. Lehmann ML, Cooper HA, Maric D, Herkenham M (2016): Social defeat induces depressive-like states and microglial activation without involvement of peripheral macrophages. *J Neuroinflammation* 13:224.

13. Russo SJ, Nestler EJ (2013): The brain reward circuitry in mood disorders. *Nat Rev Neurosci* 14:609-625.

14. Nestler EJ, Carlezon WA, Jr. (2006): The mesolimbic dopamine reward circuit in depression. *Biol Psychiatry* 59:1151-1159.

15. Golden SA, Covington HE, 3rd, Berton O, Russo SJ (2011): A standardized protocol for repeated social defeat stress in mice. *Nat Protoc* 6:1183-1191.

16. Krishnan V, Han MH, Graham DL, Berton O, Renthal W, Russo SJ, *et al.* (2007): Molecular adaptations underlying susceptibility and resistance to social defeat in brain reward regions. *Cell* 131:391-404.

17. Slattery DA, Cryan JF (2012): Using the rat forced swim test to assess antidepressant-like activity in rodents. *Nat Protoc* 7:1009-1014.

18. A J, Trygg J, Gullberg J, Johansson AI, Jonsson P, Antti H, *et al.* (2005): Extraction and GC/MS analysis of the human blood plasma metabolome. *Anal Chem* 77:8086-8094.

19. Wu MQ, Ye H, Shao C, Zheng X, Li QR, Wang L, *et al.* (2017): Metabolomics-Proteomics Combined Approach Identifies Differential Metabolism-Associated Molecular Events between Senescence and Apoptosis. *J Proteome Res* 16:2250-2261.

20. Zhang Y, Geng JL, Hong Y, Jiao L, Li SN, Sun RB, *et al.* (2019): Orally Administered Crocin Protects Against Cerebral Ischemia/Reperfusion Injury Through the Metabolic Transformation of Crocetin by Gut Microbiota. *Front Pharmacol* 10.

21. Aleyasin H, Flanigan ME, Golden SA, Takahashi A, Menard C, Pfau ML, *et al.* (2018): Cell-Type-Specific Role of Delta FosB in Nucleus Accumbens In Modulating Intermale Aggression. *J Neurosci* 38:5913-5924.

22. Labouesse MA, Lassalle O, Richetto J, Iafrati J, Weber-Stadlbauer U, Notter T, *et al.* (2017): Hypervulnerability of the adolescent prefrontal cortex to nutritional stress via reelin deficiency. *Mol Psychiatry* 22:961-971.

23. Rogers JT, Zhao L, Trotter JH, Rusiana I, Peters MM, Li Q, *et al.* (2013): Reelin supplementation recovers sensorimotor gating, synaptic plasticity and associative learning deficits in the heterozygous reeler mouse. *J Psychopharmacol* 27:386-395.

24. Rosas-Hernandez H, Cuevas E, Lantz SM, Paule MG, Ali SF (2018): Isolation and Culture of Brain Microvascular Endothelial Cells for In Vitro Blood-Brain Barrier Studies. *Methods Mol Biol* 1727:315-331.

25. Shah SH, Newgard CB (2015): Integrated metabolomics and genomics: systems approaches to biomarkers and mechanisms of cardiovascular disease. *Circ Cardiovasc Genet* 8:410-419.

26. Parker BL, Calkin AC, Seldin MM, Keating MF, Tarling EJ, Yang P, *et al.* (2019): An integrative systems genetic analysis of mammalian lipid metabolism. *Nature* 567:187-193.

27. Abouleila Y, Onidani K, Ali A, Shoji H, Kawai T, Lim CT, *et al.* (2019): Live single cell mass spectrometry reveals cancer-specific metabolic profiles of circulating tumor cells. *Cancer*

Sci 110:697-706.

28. Bergin DH, Jing Y, Mockett BG, Zhang H, Abraham WC, Liu P (2018): Altered plasma arginine metabolome precedes behavioural and brain arginine metabolomic profile changes in the APPswe/PS1DeltaE9 mouse model of Alzheimer's disease. *Transl Psychiatry* 8:108.

29. Ishizaki T, Chiba H, Kojima T, Fujibe M, Soma T, Miyajima H, *et al.* (2003): Cyclic AMP induces phosphorylation of claudin-5 immunoprecipitates and expression of claudin-5 gene in blood-brain-barrier endothelial cells via protein kinase A-dependent and -independent pathways. *Exp Cell Res* 290:275-288.

30. Soma T, Chiba H, Kato-Mori Y, Wada T, Yamashita T, Kojima T, *et al.* (2004): Thr(207) of claudin-5 is involved in size-selective loosening of the endothelial barrier by cyclic AMP. *Exp Cell Res* 300:202-212.

31. Zeisel A, Hochgerner H, Lonnerberg P, Johnsson A, Memic F, van der Zwan J, *et al.* (2018): Molecular Architecture of the Mouse Nervous System. *Cell* 174:999-1014 e1022.

32. Czysz AH, Schappi JM, Rasenick MM (2015): Lateral Diffusion of Gαs in the Plasma Membrane Is Decreased after Chronic but not Acute Antidepressant Treatment: Role of Lipid Raft and Non-Raft Membrane Microdomains. *Neuropsychopharmacology* 40:766-773.

33. Allen JA, Halverson-Tamboli RA, Rasenick MM (2007): Lipid raft microdomains and neurotransmitter signalling. *Nat Rev Neurosci* 8:128-140.

34. Segarra M, Aburto MR, Cop F, Llao-Cid C, Hartl R, Damm M, *et al.* (2018): Endothelial Dab1 signaling orchestrates neuro-glia-vessel communication in the central nervous system. *Science* 361.

35. Baeten KM, Akassoglou K (2011): Extracellular matrix and matrix receptors in blood-brain

barrier formation and stroke. *Dev Neurobiol* 71:1018-1039.

36. Fujita M, Richards EM, Niciu MJ, Ionescu DF, Zoghbi SS, Hong J*, et al.* (2017): cAMP signaling in brain is decreased in unmedicated depressed patients and increased by treatment with a selective serotonin reuptake inhibitor. *Mol Psychiatry* 22:754-759.

37. Chen X, Luo J, Leng Y, Yang Y, Zweifel LS, Palmiter RD*, et al.* (2016): Ablation of Type III Adenylyl Cyclase in Mice Causes Reduced Neuronal Activity, Altered Sleep Pattern, and Depression-like Phenotypes. *Biol Psychiatry* 80:836-848.

38. Rasenick MM (2016): Depression and Adenylyl Cyclase: Sorting Out the Signals. *Biol Psychiatry* 80:812-814.

39. Coppen AJ (1960): Abnormality of the blood-cerebrospinal fluid barrier of patients suffering from a depressive illness. *J Neurol Neurosurg Psychiatry* 23:156-161.

40. Turner CA, Thompson RC, Bunney WE, Schatzberg AF, Barchas JD, Myers RM*, et al.* (2014): Altered choroid plexus gene expression in major depressive disorder. *Front Hum Neurosci* 8:238.

41. Lehmann ML, Weigel TK, Cooper HA, Elkahloun AG, Kigar SL, Herkenham M (2018): Decoding microglia responses to psychosocial stress reveals blood-brain barrier breakdown that may drive stress susceptibility. *Sci Rep* 8:11240.

42. Gupta VK (2009): CSD, BBB and MMP-9 elevations: animal experiments versus clinical phenomena in migraine. *Expert Rev Neurother* 9:1595-1614.

43. Smagin DA, Galyamina AG, Kovalenko IL, Babenko VN, Kudryavtseva NN (2019): Aberrant Expression of Collagen Gene Family in the Brain Regions of Male Mice with Behavioral Psychopathologies Induced by Chronic Agonistic Interactions. *BioMed research*

international 2019:7276389.

44. Cope EC, Gould E (2019): Adult Neurogenesis, Glia, and the Extracellular Matrix. *Cell stem cell* 24:690-705.

45. Iafrati J, Orejarena MJ, Lassalle O, Bouamrane L, Gonzalez-Campo C, Chavis P (2014): Reelin, an extracellular matrix protein linked to early onset psychiatric diseases, drives postnatal development of the prefrontal cortex via GluN2B-NMDARs and the mTOR pathway. *Mol Psychiatry* 19:417-426.

46. Riga D, Kramvis I, Koskinen MK, van Bokhoven P, van der Harst JE, Heistek TS*, et al.* (2017): Hippocampal extracellular matrix alterations contribute to cognitive impairment associated with a chronic depressive-like state in rats. *Sci Transl Med* 9.

47. Plattner F, Hayashi K, Hernandez A, Benavides DR, Tassin TC, Tan C*, et al.* (2015): The role of ventral striatal cAMP signaling in stress-induced behaviors. *Nat Neurosci* 18:1094-1100.

48. Wray NH, Schappi JM, Singh H, Senese NB, Rasenick MM (2018): NMDAR-independent, cAMP-dependent antidepressant actions of ketamine. *Mol Psychiatry*.

49. Seligman F, Nemeroff CB (2015): The interface of depression and cardiovascular disease: therapeutic implications. *Ann Ny Acad Sci* 1345:25-35.

50. Carney RM, Freedland KE (2017): Depression and coronary heart disease. *Nat Rev Cardiol* 14.

51. Wood SK (2014): Individual differences in the neurobiology of social stress: implications for depression-cardiovascular disease comorbidity. *Curr Neuropharmacol* 12:205-211.

1

Figure legends

3

Fig. 1 Social stress vulnerability is associated with reduced cAMP specifically in the NAc

(A) Schematic representation of the CSDS procedure. (B) Stressed mice were divided into susceptible (SS) and resilient (RES) phenotypes according to the SI ratio; (C) Heat maps of time spent in the SI test. (D) Quantification of the immobile time in the TST. (E) Heat map visualizing the intensities of the metabolites that were particularly different in the NAc. (F) Level of the metabolites correlated with SI ratio; correlations were evaluated with Pearson's correlation coefficient or Spearman correlation coefficient, $*P<0.05$, $**P<0.01$. (G) cAMP levels in the NAc, PFC and Hip. (H) cAMP levels (detected by LC-MS/MS) in the NAc correlated with SI ratio and (I) cAMP levels (measured by ELISA) in the NAc correlated with SI ratio. Correlations were evaluated with Pearson's correlation coefficient. One-way ANOVA followed by Bonferroni's multiple comparison test, $*P<0.05$, $**P<0.01$, $****P<0.0001$, n.s., no significance. Data represent the mean $\pm$ s.e.m. Also see supplementary Table S1 for statistical analysis.

16

Fig. 2 cAMP supplementation improves blood-brain barrier and depressive-like behaviors

(A) Schematic representation of the CSDS procedure and M-cAMP treatment, intraperitoneally (i.p.) administered once daily 2 h prior to social defeat. (B) Individual SI ratio values. (C) 2◊2 contingency table for correlation between social avoidance and M-cAMP treatment. The numbers in the box indicate the number of animals. Fisher's exact test, $P=0.0033$. (D) Quantification of the immobile time in the TST and FST (E). The plasma (F) and NAc (G) cAMP levels after a single

1 i.p. M-cAMP treatment (n=6), two-way ANOVA followed by Bonferroni's multiple comparison

2 test, ***$P<0.001$, ****$P<0.0001$, n.s., no significance. (H) Quantification of the Cldn5 expression,

3 ratio of Cldn5$^+$ area/CD31$^+$ area. (I) Representative costaining with CD31 and Cldn5 in blood

4 vessels. Scale bars, 20 μm. (J) Schematic representation of the CSDS procedure and M-cAMP

5 treatment. (K) Assessment of BBB permeability with Evans Blue dye. (L) Individual SI ratio

6 values on different days. (M) Quantification of the immobile time in the TST and FST (N).

7 One-way ANOVA followed by Bonferroni's multiple comparison test, *$P<0.05$, **$P<0.01$,

8 ***$P<0.001$, ****$P<0.0001$, n.s., no significance. Data represent the mean±s.e.m. Also see

9 supplementary Table S1 for statistical analysis.

10

11 **Fig. 3 cAMP is markedly decreased in neurons in the NAc of stress-susceptible mice**

12 cAMP levels in vascular segments (A) and myelin debris (B) in the NAc. Right: cAMP level

13 correlated with SI ratio. Correlations were evaluated with Pearson's correlation coefficient. (C)

14 Co-staining of the NAc with cAMP and β3-tubulin (neurons), GFAP (astrocytes), and Iba1

15 (microglia). Scale bars, 50 μm. Scale bars of insets: 20 μm. Staining intensity was quantified (D),

16 and colocation analysis was performed (E) as shown in the right panels. (F) mRNA expression of

17 different isoforms of adenylyl cyclase in the NAc of mice. Protein expression of Adcy5 and Gsα in

18 the nonlipid raft (G) and lipid raft regions (H). n = 8 experimental replicates/group, and the

19 statistics are shown in the lower panels. One-way ANOVA followed by Bonferroni's multiple

20 comparison test, *$P<0.05$, ***$P<0.001$, ****$P<0.0001$. n.s., no significance. Data represent the

21 mean±s.e.m. Also see supplementary Table S1 for statistical analysis.

22

1 **Fig. 4 Behavioral changes following endogenous modulation of neuronal cAMP synthesis in**

2 **the NAc**

3 (A) Schematic representation of the Adcy5 rescue experiment. (B) Individual SI ratio values on

4 day 29. (C) Quantification of the immobile time in the TST on day 30. (D) Individual SI ratio

5 values on day 38. (E) Quantification of the immobile time in the TST on day 39. (F) Assessment

6 of sucrose preference on day 41. (G) Schematic representation of the cAMP replenishing

7 experiment. (H) Individual SI ratio values on day 29. (I) Quantification of the immobile time in

8 the TST on day 30. (J) Individual SI ratio values on day 38. (K) Quantification of the immobile

9 time in the TST on day 39. (L) Assessment of sucrose preference on day 41. Two-way ANOVA

10 followed by Bonferroni's multiple comparison test, *$P<0.05$, **$P<0.01$, ****$P<0.0001$. Data

11 represent the mean$\pm$s.e.m. Dox, doxycycline. Also see supplementary Table S1 for statistical

12 analysis.

13

14 **Fig. 5 Reelin mediates the antidepressant-like effects of cAMP**

15 mRNA (A) and protein (B) expression of reelin in the NAc of AAV-shRNA and

16 AAV-shRNA-Adcy5 mice. Scale bars, 200 μm. Scale bars of insets: 30 μm. Unpaired *t*-test with

17 equal variance, *$P<0.05$. (C) Colocalization of biotinylated IL-6 and CD31 in the NAc. Scale bars,

18 20 μm. (D) Schematic representation of the reelin replenishing experiment. (E) Individual SI ratio

19 values of mice. (F) Heat maps of time spent in the SI test. (G) Assessment of sucrose preference.

20 (H) Colocalization of biotinylated IL-6 and CD31 in the NAc. Scale bars, 20 μm. (I) Protein

21 expression of reelin after acute fluoxetine treatment. (J) Protein expression of reelin after chronic

22 fluoxetine treatment. The statistics are shown in the bottom panels. Two-way ANOVA followed by

1   Bonferroni's multiple comparison test, *P*<0.05, **P*<0.01. n.s., no significance. Data represent

2   the mean±s.e.m. Also see supplementary Table S1 for statistical analysis.

A
Reelin mRNA fold change

● AAV-shRNA
● AAV-shRNA-Adcy5

B
AAV-shRNA   AAV-shRNA-Adcy5
Reelin

C
Unstressed AAV-shRNA   Stressed AAV-shRNA   Unstressed AAV-shRNA-Adcy5   Stressed AAV-shRNA-Adcy5
CD31
IL-6-biotin
DAPI

D
AAV-shRNA
AAV-shRNA-Adcy5
Micro-defeat
Behavioral tests
1 Surgery   14 Dox   28 Reelin   32   36 Tissue collection

E SI Test
SI ratio
P=0.09
Unstressed   Stressed

F
AAV-shRNA   AAV-shRNA-Adcy5
Unstressed
Stressed
Time spent

G SPT
Sucrose preference (%)
□ AAV-Adcy5
■ AAV-Adcy5+Reelin
Unstressed   Stressed

H
Unstressed AAV-shRNA-Adcy5 +Saline   Unstressed AAV-shRNA-Adcy5 +Reelin   Stressed AAV-shRNA-Adcy5 +Saline   Stressed AAV-shRNA-Adcy5 +Reelin
CD31
IL-6-biotin
DAPI

I
CTRL   SS
Reelin
β-actin
Saline   +   -   +   -
Fluoxetine   -   +   -   +
Relative Reelin protein level
○ Saline ● Fluoxetine
CTRL   SS

J
CTRL   SS   MW kDa
Reelin   -388
β-actin   -42
Saline   +   -   +   -
Fluoxetine   -   +   -   +
Relative Reelin protein level
□ Saline ■ Fluoxetine
n.s.
CTRL   SS